FMCW Differential Synthetic Aperture Ladar for Turbulence Mitigation

Zeb W. Barber (a), Jason R. Dahl, and Christopher Ross Blaszczyk
(a) Montana State University, Spectrum Lab
PO Box 173510 Bozeman, MT 59717
barber@spectrum.montana.edu

Abstract: Synthetic Aperture (SA) imaging, including holographic aperture ladar (HAL), synthetic aperture ladar (SAL), and combinations thereof; are promising solutions for long range imaging applications. One of the major difficulties with real-world SA imaging is coherently processing the image information in the presence of atmospheric turbulence. Differential SAL imaging was proposed and patented in 2005 as a technique to reduce the sensitivity of synthetic aperture imaging ladar to line-of-sight motion errors and shown to reduce sensitivity to dynamic turbulence near the target. We will present experimental laboratory demonstrations of high range resolution DSAL with comparisons of performance to standard SAL processing in the presence of localized dynamic turbulence. Our DSAL receiver is based on imaging the receive aperture and LO onto quad-cell detectors that measure the ladar signal in each quadrant of the aperture separately. We will also discuss how differential techniques can mitigate atmospheric turbulence with other SA imaging techniques.

Keywords: Coherent Laser Radar, Synthetic Aperture Imaging

1. Introduction

By exploiting the relative motions of the transmitter (Tx), receiver (Rx), and/or target Synthetic Aperture Ladar (SAL) imaging techniques have the ability to provide image resolution beyond the standard diffraction limited resolution of the physical optical aperture[1]. Two key requirements for SAL imaging are: a coherent laser radar system that provides range resolution commensurate with the desired image resolution, and robust techniques to correct and compensate for the inevitable phase errors that arise during the aperture/object motion. Our high resolution (< 0.5 cm) frequency modulated continuous wave (FMCW) ladar systems[2], [3], allow us to study SAL imaging at short ranges in a laboratory environment. This has the advantage of eliminating many engineering and fundamental challenges found in long-distance SAL imaging such as high power lasers, beam steering and pointing stability, and uncontrollable atmospheric turbulence, allowing us to focus on the imaging techniques.

Despite eliminating many challenges, controlling aperture motion and phase errors in the ladar system to much better than the optical wavelength is impractical so one still needs to utilize data based phase error compensation. We have found that the phase gradient autofocus algorithm (PGA), which was developed for radar imaging, is very successful at compensating phase errors for most SAL imaging situations even when the pulse-to-pulse common mode phase error exceeds$\pm\pi$. The success of the PGA algorithm is based on its fantastic ability to provide optimal estimates of the common mode piston phase error for high clutter and/or low SNR situations, even including low light levels where the average image brightness is on the order of a few photons per pixel[4]. Combining our high range resolution FMCW ladar sources and straightforward use of the PGA algorithm we have successfully investigated many SAL imaging modalities with table-top experiments including: stripmap modes, spotlight modes, bistatic modes, interferometric SAL, etc. [5].

For real-world SAL imaging scenarios atmospheric turbulence presents challenges different than with other imaging methods. In general, atmospheric turbulence causes no blurring in range dimension. (However, for FMCW ladars that utilize long pulses ($\gg 10$ µs), range blurring can be observed for atmospheres with high Greenwood frequencies due to the Doppler effect.) Thus, the effects of the turbulence on SAL imaging are mainly observed in the cross-range dimension. One advantage of SAL is that due to the ability to correct the phase using PGA or other methods, important scaling of the atmospheric coherence diameter, r_0, is to the real-aperture as opposed to the full synthetic aperture size. In terms of thin phase screens at different locations, a phase screen located near the Tx/Rx optics generates mainly common mode pulse-to-pulse phase errors and are well corrected by the PGA algorithm as long as the r_0 is larger than the real aperture. This applies even if the atmospheric coherence time is smaller than the total SAL collection time. A thin phase screen near the target that is static over the total SAL collection time merely amounts to an added phase distortion of the image, which has little effect on the intensity image. However, if the phase screen near the target is not static then the phase evolution for different areas of the target will not be common mode and the PGA estimate will be corrupted and insufficient to compensate all areas of the target image simultaneously. This is roughly equivalent to anisoplanatic errors. For a turbulent phase screen in between the target and the Tx/Rx optics there will be combinations of common mode and anisoplanatic errors.

Differential SAL (DSAL) is a hardware based technique to compensate pulse-to-pulse phase errors that was proposed and patented by Stappaerts & Scharlemann in 2005[6], [7]. The basic concept behind DSAL is to measure the derivative of the received ladar signal phase across real aperture rather than the actual field phase. The benefit is that this derivative is insensitive to common mode phase fluctuations caused by relative motion between the aperture and the object. The derivative can then be numerically integrated across the synthetic aperture dimension to recover the full phase evolution up to an overall phase. In the Stappaerts and Scharlemann paper they outline a 1D scheme and algorithm that calls for dividing the Rx aperture, d, into two subapertures and separately measuring the phase in the left and right halves for each SA step of $d/4$. In the paper, it is shown that for steps of $d/4$ the field in one subaperture is identical to that of the other in the previous step (i.e. one subaperture lags the other by one step). This means the differential phase, $\Delta\varphi_i = \varphi_{r_i} - \varphi_{l_i}$, between the left and right halves can simply be cumulatively summed to generate a recovered phase evolution, $\tilde{\varphi}_i$, rather than having to scale the phase according to the step size. This phase is then combined with the field amplitude from one subaperture to generate a recovered field measurement, which is then processed with the standard SAL processing.

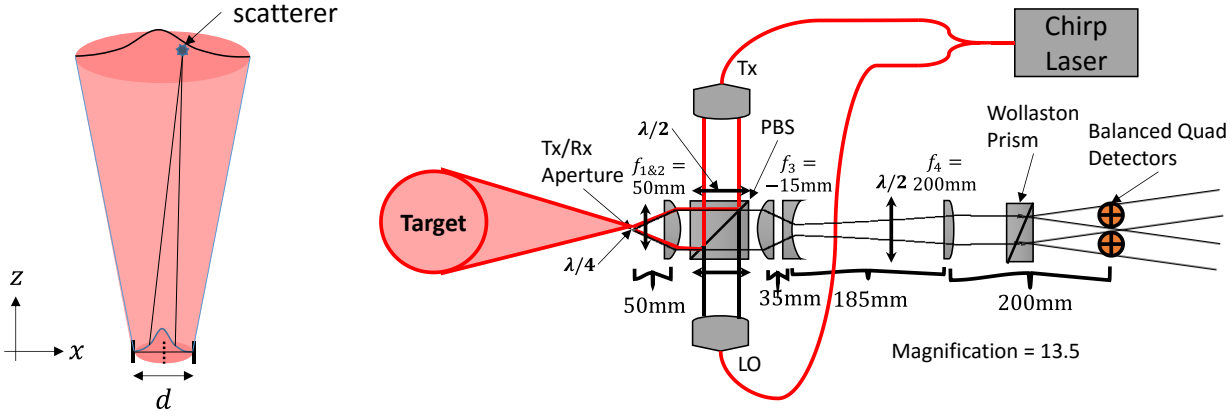

Figure 1. (Left) Differential SAL (DSAL) concept diagram. (Right) DSAL receiver design.

It is clear that the DSAL method is insensitive to piston phase fluctuations due to atmospheric turbulence, however Ref [6] makes a claim: "DSAL, unlike SAL, is not affected by turbulence changes near the target." This claim is what motivated our interest in investigating the DSAL technique. If true the DSAL would have a distinct advantage over SAL + PGA phase compensation for long rang SAL imaging

applications. We report here our construction and testing of a high resolution laboratory DSAL imaging system including testing of performance in comparison to SAL + PGA for different turbulence conditions.

2. DSAL Design and Experimental Results

The design goal of our DSAL system (see Figure 1), was a monostatic system that would have reconfigurable Tx/Rx apertures and beams and a convenient method of separating the measurements in the subapertures. To accomplish a reconfigurable Tx/Rx aperture, the system uses a lens to focus the Tx beam, collimated out of the fiber coupled chirp source, to create a "virtual" Tx aperture. For the experiments shown here a 50 mm focusing lens is used to create a ~35 μm spot. This provides a sufficiently large illumination spot at the target ~20 cm so that good sized (greater than 100 x 100) SAL images could be formed with our ~2 mm resolution FMCW ladar system. The subaperture formation is accomplished by use of a quad-cell detector as the receiver, which allows us to divide the aperture into quadrants. This detector has a diameter of 1 mm, which for our short range measurements is much too large to sample the field in the aperture plane, so the optical design provides a magnification of ~13.5 for a 50 mm focusing lens. The Rx aperture is defined both by the image of the quadcell detector and the soft "virtual" Rx aperture defined by the LO beam. The LO and Rx mixing is accomplished using balanced polarization based mixing and the balance is achieved by photocurrent subtraction with a second quad-cell detector. The quad-cell detector circuit is a Hobb's type auto-balancing detector and generates four balanced outputs – one for each quadrant. The four outputs are digitized with an 8 channel, 12 bit, 80 MS/s digitizer from PicoTechnology. The DSAL Tx/Rx optics and detector have been constructed using optical cage hardware on an optical breadboard that is then mounted onto a computer controlled motorized linear stage to provide aperture motion. For our short distances only small synthetic apertures < 1 cm are required to achieve cross-range resolution commensurate with the ladar range resolution.

The target for these investigations was homemade using 3M Diamond retro-reflecting tape (for high return signal) on a black background in a pattern of triangles and bars. Placed at a distance of 5 to 8 m. Atmospheric turbulence was applied by placing a space heater below the propagation path. This generates very strong turbulence at an estimated level of $C_n^2 \leq 10^{-10}$. Both the DSAL and SAL+PGA processing start from the range compressed data $S_q(r_p, x_j)$, where the subscripts j, p, q refer to SA aperture domain, the image domains, and the quadrant of the detector, respectively. For the SAL+PGA processing the PGA algorithm is implemented starting with an estimated PSF window function that spans the whole image and slowly decreases by 10% until the phase error estimate converges to less than $\pi/10$. The SAL+PGA image quality is nearly identical using a single detector or by summing the signals from each detector before applying PGA. The DSAL processing starts with $S_q(r_p, x_j)$ for each quadrant and makes an estimate of the field from the right and left half detectors as:

$$\exp\{i\varphi(r_p, x_j)\} = \prod_{k=1}^{j} \exp\left\{\left(i v_x \delta_x \angle\left[\left(S_1(r_p, x_k) + S_4(r_p, x_k)\right)\left(S_2(r_p, x_k) + S_3(r_p, x_k)\right)^*\right]\right)\right\}, \quad (1)$$

where the δ_x is the SA step size, v_x is a scaling factor for the step size relative to the size of the Rx aperture (nominally $4/d$ for the DSAL collection defined in Ref. [6]). The product accomplishes the integration of the differential phase across the synthetic aperture. This is then multiplied by the sum of the field amplitudes as $S_{DSAL} = \left(\sum_q |S_q(r_p, x_j)|\right) \exp\{i\varphi(r_p, x_j)\}$, and then compressed in the cross-range dimension with the proper quadratic phase compensation for the collection geometry.

Figure 2 compares the resulting DSAL and SAL+PGA images for different placements of the space heater (and no heater). From these images we make several observations: First, the DSAL images show significant errors where the image is wide. We believe that this is due to the limited magnification of the Rx aperture onto the quadrature detector, which tends to low pass filter the estimate of the differential phase in the aperture plane, corrupting the phase estimate for the high cross-range frequencies. Higher magnification or use of a hard aperture stop at the Tx/Rx aperture plane could provide improvement. Second, with no

turbulence the sharpness of SAL+PGA processed image is sharper than that of the DSAL image, pointing toward a better estimate of the common mode phase errors. This effect was dependent on the image brightness, indicating that the differential phase estimate is relatively sensitive to signal noise including shot-noise. Third, the cross-range position of the SAL+PGA images is not stable. We have found that the PGA algorithm tends to shift the image in cross-range as this does not affect the width of the average PSF, which is what the PGA tries to optimize. Fourth, the DSAL processing tends to degrade more gracefully in the presence of turbulence particularly when the turbulence is nearer to the target. The SAL+PGA processing degrades by reducing the image contrast, whereas the DSAL processing losses resolution and tends to converge toward the auto-correlation function.

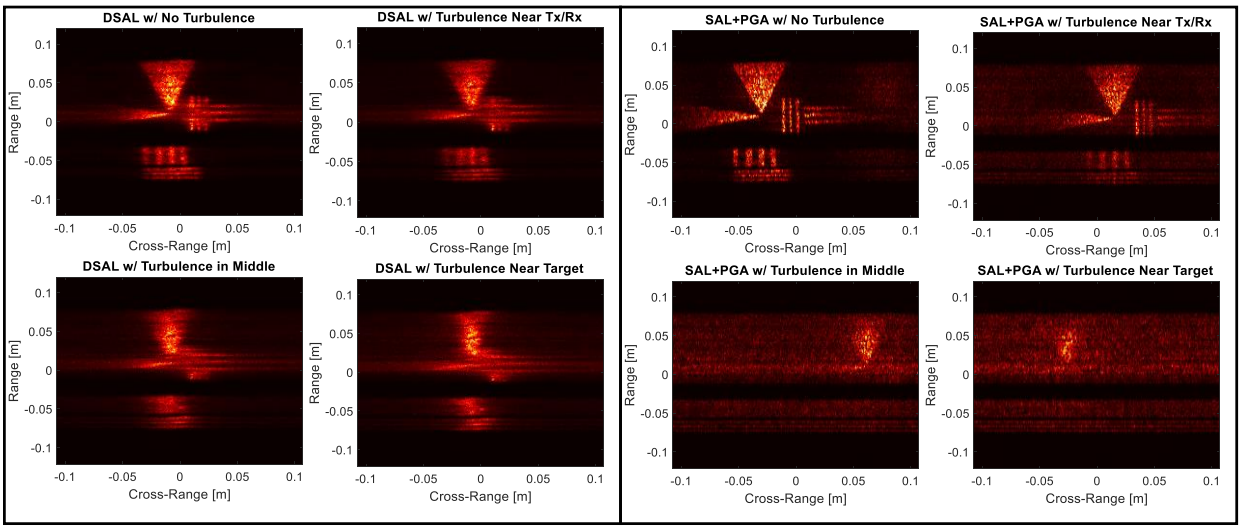

Figure 2. Comparison of DSAL and PGA+SAL for different locations of turbulence.

3. Discussion

While the experimental evidence here shows that DSAL appears more robust to turbulence near the target than SAL+PGA, turbulence near the target has a much larger effect on the DSAL than turbulence near the Tx/Rx. Further investigation shows that for targets with a single point scatterer per range line, DSAL does provide immunity from turbulence near the target as separate estimate of the piston phase is made for each range. However, fundamentally the presence of multiple scatterers in the cross-range direction with uncorrelated turbulence (i.e. separation $> r_0$) mixes these phase errors in the differential phase estimates leading to cross-range blurring. Despite this lack of immunity, the DSAL method is still attractive as it is much less processing intensive than PGA and thus merits further research.

4. References

[1] B. W. Krause, J. Buck, C. Ryan, D. Hwang, P. Kondratko, A. Malm, A. Gleason, and S. Ashby, "Synthetic aperture ladar flight demonstration," in *2011 Conference on Lasers and Electro-Optics (CLEO)*, 2011, pp. 1–2.

[2] P. A. Roos, R. R. Reibel, T. Berg, B. Kaylor, Z. W. Barber, and W. R. Babbitt, "Ultrabroadband optical chirp linearization for precision metrology applications," *Opt. Lett.*, vol. 34, no. 23, p. 3692, Nov. 2009.

[3] N. Satyan, A. Vasilyev, G. Rakuljic, V. Leyva, and Amnon Yariv, "Precise control of broadband frequency chirps using optoelectronic feedback," *Opt. Express*, vol. 17, 2009.

[4] Z. W. Barber and J. R. Dahl, "Synthetic aperture ladar imaging demonstrations and information at very low return levels," *Appl. Opt.*, vol. 53, no. 24, pp. 5531–5537, Aug. 2014.

[5] S. Crouch and Z. W. Barber, "Laboratory demonstrations of interferometric and spotlight synthetic aperture ladar techniques," *Opt. Express*, vol. 20, no. 22, pp. 24237–24246, Oct. 2012.

[6] E. A. Stappaerts and E. T. Scharlemann, "Differential synthetic aperture ladar," *Opt. Lett.*, vol. 30, no. 18, pp. 2385–2387, Sep. 2005.

[7] E. A. Stappaerts, "Differential optical synthetic aperture radar," US6879279 B2, 12-Apr-2005.